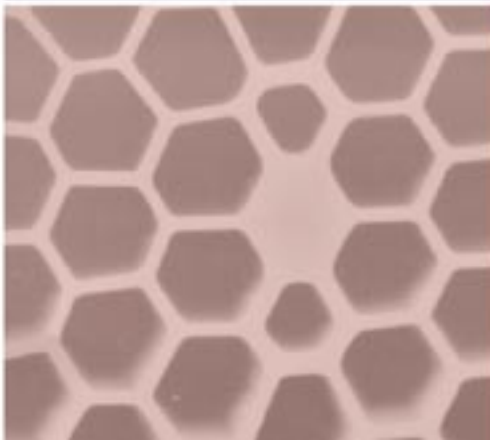
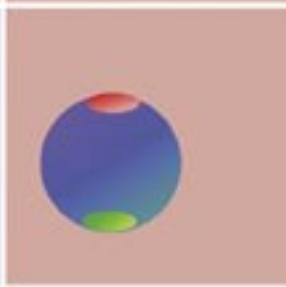
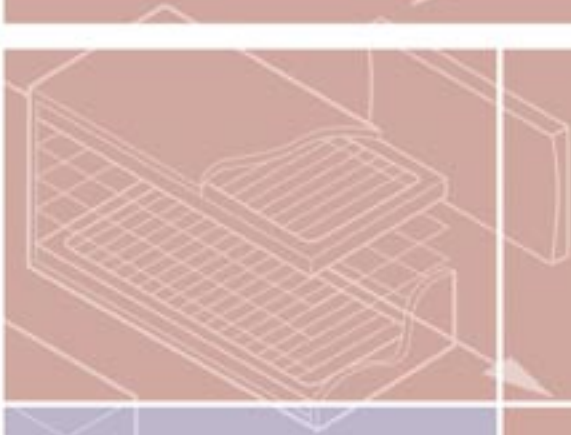
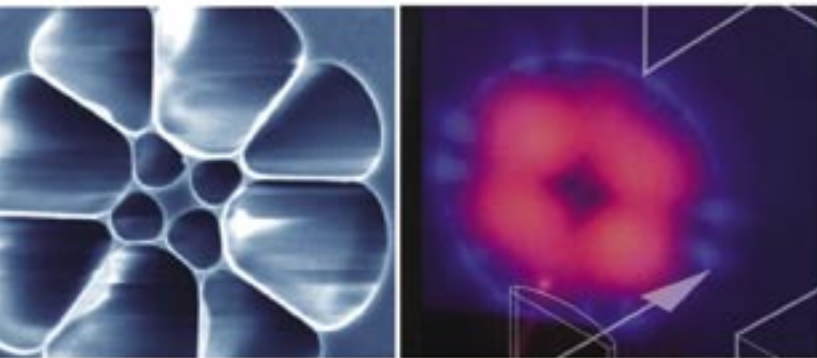
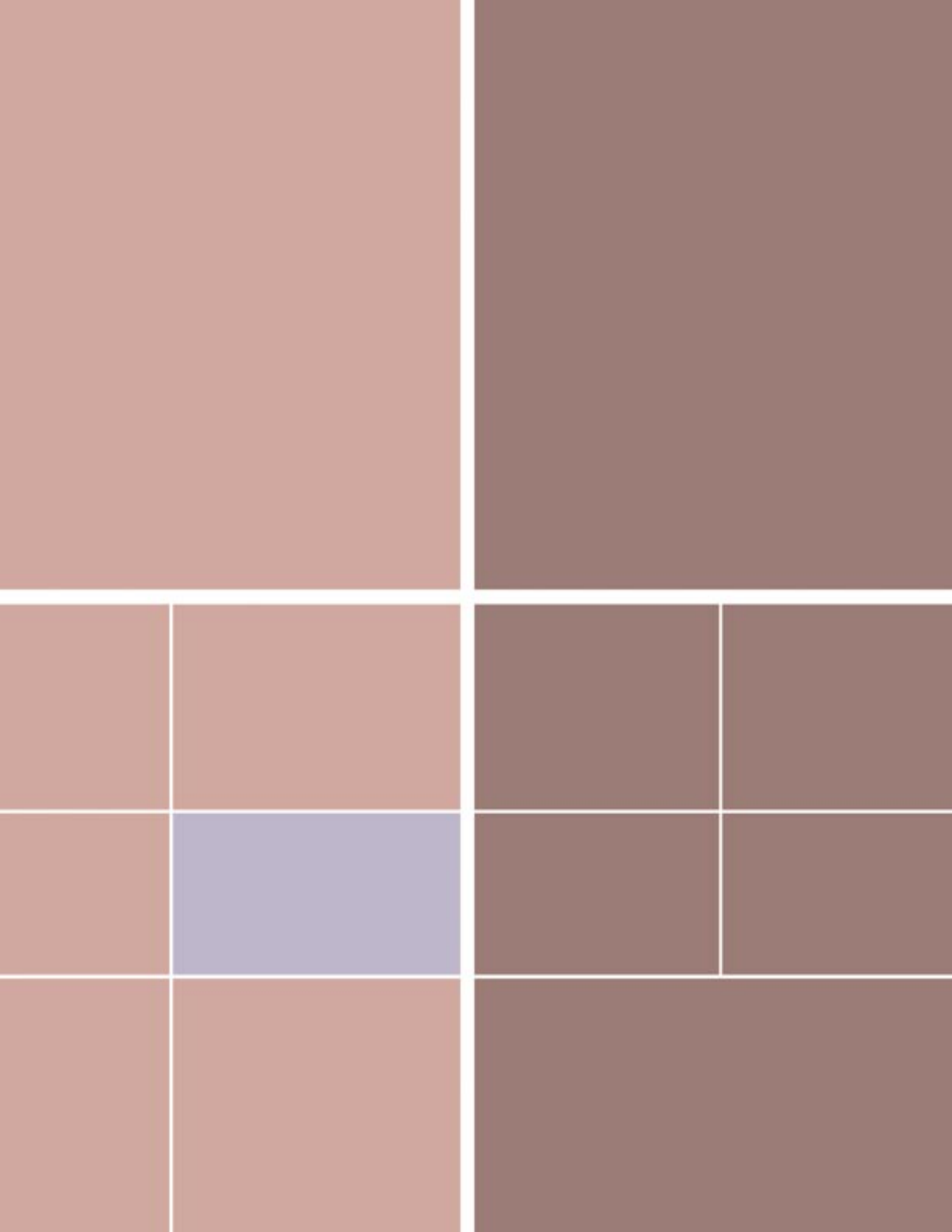


*Atomic Physics  
Research Highlights*





# Quantum Simulations of Condensed Matter Systems using Trapped Ions

D.J. Berkeland, G.H. Ogin, W.R. Scarlett (P-21), M.G. Blain, C.P. Tigges (SNL)

When Richard Feynman famously proposed a quantum computer, his intended application was actually to simulate quantum dynamical systems. This problem is difficult because as the number of elements of a quantum system increases *linearly*, the complexity of the equations modeling it grows *exponentially*. For example, to completely describe the dynamics of just 40 spin-1/2 particles requires  $2^{40} \times 2^{40} = 10^{24}$  matrix elements, orders of magnitude greater than what can be stored on any classical supercomputer. This complexity is why we cannot even determine the correct theoretical behavior of some important systems. Our understanding of quantum phenomena such as superconductivity, antiferromagnetism, behavior of *f*-electrons in solids, and so on, is seriously limited.

Feynman's proposed solution to this problem was to simulate one quantum-mechanical system with another. The states of the simulator would follow the same equations of motion as the real system, yet would be directly accessible so the state evolution could be monitored. A decade later, Seth Lloyd showed that Feynman's conjectured solution was correct. He pointed out that "a mere 30 or 40 quantum bits would suffice to perform quantum simulations of multidimensional fermionic systems such as the Hubbard model," which is believed to explain phenomena such as high-temperature superconductivity, "that have proved resistant to conventional computational techniques."<sup>1</sup>

A first-principles understanding of the behavior of materials would profoundly affect academia, defense, and industry. In spite of this, little experimental effort has been extended towards quantum simulations of condensed-matter systems. This is because theoretical proposals for quantum simulations have been cast in general terms. Only recently, quantum information theorists have begun to map these problems onto experimentally accessible atomic systems, urged on by correspondingly recent advances in coherent manipulations of those systems. For example, E. Jané proposed that several paradigms of condensed-matter physics can be modeled in trapped-ion systems and neutral atoms in optical lattices.<sup>2</sup> Subsequently, more detailed simulations were proposed for trapped ions in Porras' and Barjaktarevic's studies.<sup>3,4</sup>

These proposals rely on several key concepts. A single atom can simulate a spin system (for example, an electron) which is the fundamental building block of real material. Laser light interacts with the atoms to simulate site-specific potentials (such as magnetic fields). State-dependent optical forces manipulate atomic positions to simulate interactions between the spin systems. Put together, these components map atomic systems onto equivalent arrays of quantum spins found in some condensed-matter systems. Yet, our atomic

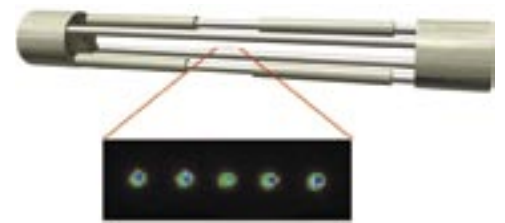


Figure 1. Our current ion trap and a depiction of five ions confined along its axis. The picture below the trap shows five ions imaged in our laboratory.

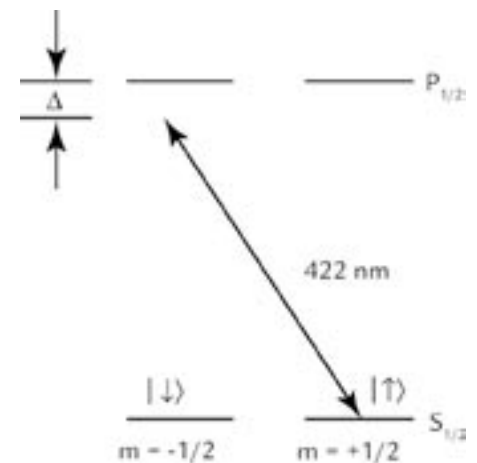


Figure 2. Relevant energy levels and optical transition in strontium-88(+). The  $S_{1/2}$  states simulate a spin-1/2 system, and the near-resonant 422 nm light creates the state-dependent force described below.

## RESEARCH HIGHLIGHT PHYSICS DIVISION

## Atomic Physics Research Highlights

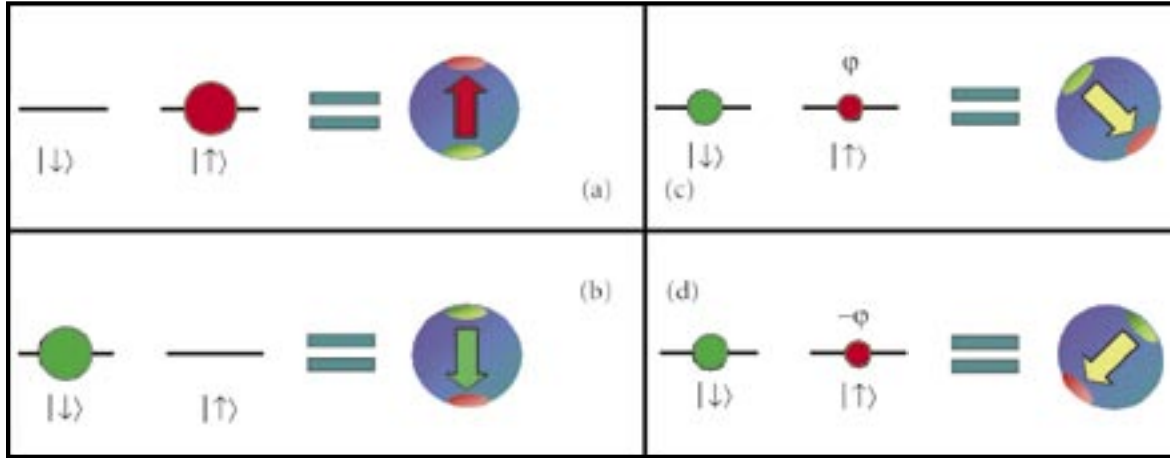


Figure 3. Simulated spin and its direction. In (a) the ion is in the  $|\uparrow\rangle$  state and the spin points “up”; in (b) the ion is in the  $|\downarrow\rangle$  state and the spin points “down”; in (c) the ion is in a superposition of states and its dipole points in a corresponding direction; in (d) the phase of the  $|\uparrow\rangle$  component is reversed and the spin is rotated relative to (c).

spin systems can be free of complicating impurities and defects, we can precisely control the interatomic interactions, and the system evolution can be characterized and measured more easily than in real materials.

We will describe experiments we are just beginning, using arrays strontium-88(+) ions confined in our linear radio-frequency trap.<sup>5</sup> This work is part of a larger LANL project on quantum simulations in Theoretical Division and Chemistry Division.

### Basic Interactions

We confine ions in the trap shown in Figure 1. Figure 2 shows the relevant optical transition and quantum-mechanical states of strontium-88(+). The Zeeman levels of the ion’s ground state simulate the spin-up and spin-down states of a spin-1/2 particle:  $|\downarrow\rangle = |S_{1/2}, m_J = -1/2\rangle$  and  $|\uparrow\rangle = |S_{1/2}, m_J = +1/2\rangle$ . The ion’s wavefunction is described by the equation  $\psi = c_\uparrow |\uparrow\rangle + c_\downarrow |\downarrow\rangle$ , where  $c_\uparrow$  and  $c_\downarrow$  are complex numbers with a relative phase  $\phi$  between them. We can determine  $\psi$  using a series of laser and magnetic-field pulses not described here. As Figure 3 illustrates, this spin system of  $|\downarrow\rangle$  and  $|\uparrow\rangle$  states can be visualized as a vector. The vector’s direction depends on the relative probability of the ion being in one state

or the other and on the phase difference between  $c_\uparrow$  and  $c_\downarrow$ .

Figure 4 illustrates how we induce ion-ion interactions that simulate the spin-spin interactions in condensed-matter problems. A force on each ion pushes it in the  $\alpha$  direction only if it is in the  $|\uparrow\rangle_\alpha$  state ( $|\uparrow\rangle$  in the basis in which  $\alpha$  is the quantization axis). We derive this force from beams of 422 nm laser light that are tightly focused on points a few microns from each ion in the  $z$ -direction. This light is detuned  $\Delta = 1$  to 10 GHz below resonance with the  $S_{1/2} \leftrightarrow P_{1/2}$  transitions as shown in Figure 1. This detuning  $\Delta$  is enough that spontaneously scattered light does not ruin the coherence between the spin states, but not so much that the laser no longer affects the ion. The atom-laser interaction creates an optical dipole force so that the ion moves towards the most intense part of the laser beam. Furthermore, the light is circularly polarized so that the  $|\uparrow\rangle$  takes part in the atom-light interaction, but not the  $|\downarrow\rangle$  state. If the ion is in a superposition of the  $|\downarrow\rangle$  and  $|\uparrow\rangle$  states, only its  $|\uparrow\rangle$  component moves along the  $z$ -axis. This part of its wavefunction accumulates a phase  $\phi$  because it moves through the combined potential of the trap and the other ions.<sup>6</sup> Changing the relative phase between the  $|\downarrow\rangle$  and  $|\uparrow\rangle$  wave-function components is equivalent to rotating the simulated spin

about the  $z$ -axis. Because this rotation depends on the relative positions of the other ions in the trap, and because the state-dependent force of 422 nm laser beams also affects those positions, the rotation angle of one spin-1/2 system depends on the quantum states of the other ions.

It is not surprising, then, that these interactions result in a spin-spin interaction term in the equations describing this system. More rigorous calculations show that the interactions due to the 422 nm pushing laser can map onto the Ising model (in which just the vertical components of the particles’ spins interact), and the XYZ model (in which all three components of spins interact) if three sets of 422 nm beams propagate along the three orthogonal trap axes.<sup>3</sup> These two models describe some of the most fundamental interactions in quantum many-body systems, from which many more complicated systems can be derived.

### Quantum Simulations

All of our simulations will follow a similar basic procedure. The system will be initialized so that all ions are in the  $|\downarrow\rangle$  state. The lasers will then be turned on for up to  $\sim 100 \mu\text{s}$ . After this process, we will measure the state of each ion. As an

example, we could search for a quantum phase transition in a one-dimensional array of trapped ions as the simulated spin-spin interaction grows relative to an applied magnetic field. At a particular value, we expect that the final state of the ion array changes from a disordered one to either one in which the spins are aligned with each other, or one in which the direction of the spins alternate along the ion array.

We can compare our experimental results to exact calculations when we use small numbers of ions and two sophisticated computer simulations using somewhat larger systems. This comparison of moderately large physical systems with computational results will let us check the precision of our experimental system and that of our theoretical techniques as they progress together. However, even the most sophisticated computer approximations cannot simulate the dynamics of one-dimensional systems with more than roughly 30 spins, and we expect to be able to perform such experiments in the next few years.

Two-dimensional arrays of trapped ions will allow more sophisticated and complex simulations. A good first choice for a two-dimensional spin array is a two-legged ladder such as that shown in Figure 5. Inducing XYZ and Ising interactions on such a ladder will let us investigate systems that display unusual phase transitions and systems that have possible connections to high- $T_c$  superconductivity.<sup>7</sup> In fact, we can make the interactions between opposite spins of a spin ladder XY-like, while coupling nearest neighbor spins with an Ising-like interaction. The resulting quantum-spin model is equivalent to a one-dimensional fermionic Hubbard model.<sup>8</sup> This is the most widely used model of a strongly interacting system in condensed-matter physics, and the ability to simulate it vastly increases our ability to use our simulator to understand materials-science problems.

Through collaboration between LANL and Sandia National Laboratories, we are designing the new ion traps that are

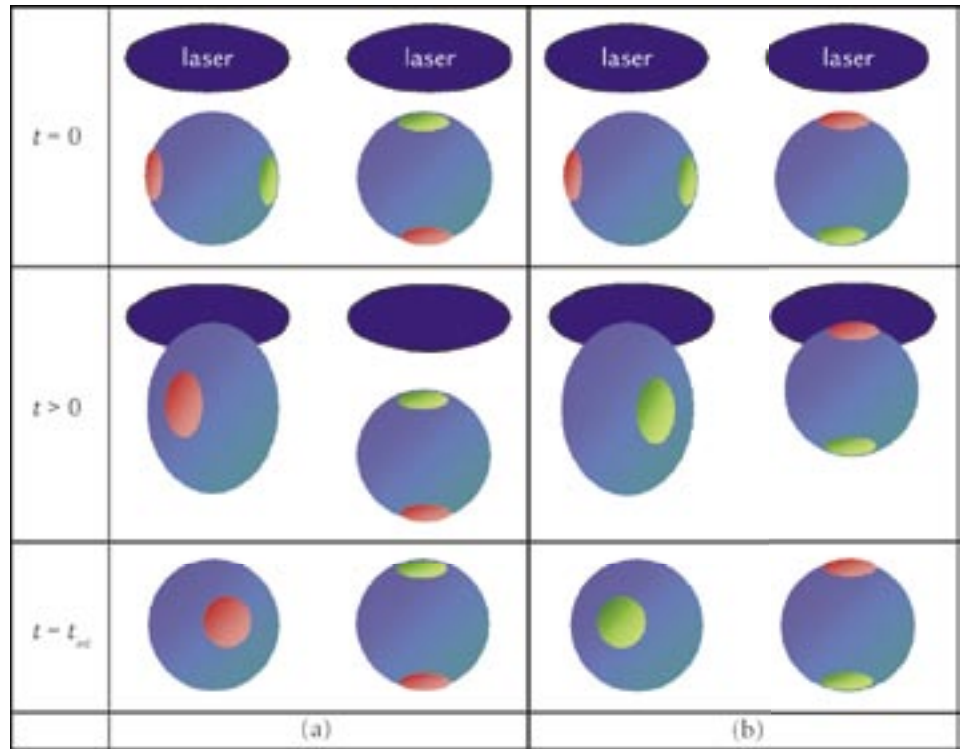


Figure 4. Effect of the 422 nm laser beam on the direction of the atomic spin depends on the state of the ion and that of the ions next to it. At  $t = 0$ , the 422 nm laser beams are turned on. In (a), the ion on the right is in the  $|\downarrow\rangle$  state and not affected by the laser beam, but it is pushed downward due to the Coulomb repulsion from the ion on the left. In (b), the ion on the right is in the  $|\uparrow\rangle$  state and is pulled toward the beam center. In both (a) and (b), the ion on the left sees its  $|\uparrow\rangle$  component pulled into the laser beam. But in (a), its  $|\uparrow\rangle$  component sees a phase shift  $\phi$  as it moves through the Coulomb field of the other ion, while in (b), its  $|\downarrow\rangle$  component feels almost the same shift  $\phi$  as the other ion moves relative to it. So, when the 422 nm light is turned off at  $t = t_{int}$ , the ion in (a) has rotated by nearly the opposite amount as the ion in (b). This quantum gate operation, in which the final state of one ion depends on the quantum state of its neighbor, simulates interaction terms found in quantum condensed-matter systems.

required for simulations with tens of ions in one and two dimensions. Such traps will be microfabricated in a unique tungsten deposition process that has already made arrays of millions of micron-sized ion traps for mass-spectroscopy applications.<sup>9</sup> We will push this process to build the first two-dimensional traps, to confine two parallel, interacting ion chains (a spin ladder), and to confine ions in configurations

such as a hexagonal close-packed array. These microfabrication techniques can build traps that are compatible with the trap-mounted photonics, electronics, and data-acquisition systems that will be necessary for our quantum simulations with larger ion arrays.

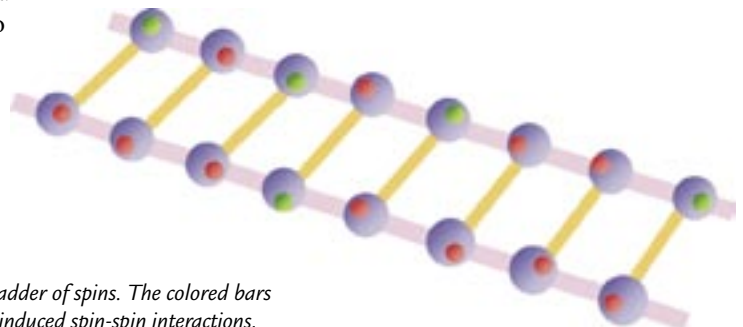


Figure 5: A two-legged ladder of spins. The colored bars represent different laser-induced spin-spin interactions.

## Atomic Physics Research Highlights

### Impact on Other Fields

What will we gain from these experiments? We have already described the sorts of first-principle understandings into materials science resulting from these physical simulations. These insights should lead to practical advances in real materials science. Historically, the ability to design and manufacture better materials has been crucial to military and industrial superiority. Developing such materials in fabrication labs with macroscopic samples is extremely expensive and time consuming, and investigating them in scientific labs is difficult because of imperfections and complications in real materials. Because of this, massive computational resources are applied to these problems, but these techniques falter when quantum-mechanical effects become important. A quantum simulator could ultimately be used to design advanced materials with new types of quantum-mechanical order. Even without using thousands of simulated spins, a quantum simulator could test the models that are used in the design of advanced materials before designers fully invest their funding and time.

Another significant benefit from these experiments is that they will represent the largest quantum computer test-bed to date. This special class of quantum computers is experimentally feasible because the stringent requirements of universal quantum computation are drastically reduced, largely because the interactions are simple and fast. The quantum simulator requires less laser stability than a universal quantum computer and less immunity from the external field noise that destroys quantum mechanical entanglement. The ions do not have to be prepared in their ground state of motion.<sup>3,6</sup> Indeed, the extreme demands of error correction on

quantum computing are vastly reduced and probably unnecessary for simulations involving 30–50 ions.<sup>10</sup> Consequently, we can leap from studying one and two ions for universal quantum computation to working with an order of magnitude more ions in more than one dimension. We therefore expect to gain crucial insight into the engineering and algorithmic demands of large-scale quantum computation.

Finally, even though a quantum simulator requires much less control over a physical system than a quantum computer does, it still uses the same technical resources. Both applications require traps that can hold large, two-dimensional arrays of ions. Both will ultimately require complex optical systems and compact data-acquisition systems that can function with thousands of ions, or more, simultaneously. Because the two systems share common needs, the technology developed while building a quantum simulator would lead to practical quantum computation.

In short, the work described here has the fortunate attributes of both basic, fundamental science and practical, applied technologies. We expect to contribute both to national-security interests and to the intellectual pursuits of condensed-matter and quantum-information scientists.

### References

1. S. Lloyd, "Universal quantum simulators," *Science* **273**, 1073–1078 (1996).
2. E. Jané *et al.*, "Simulation of quantum dynamics with quantum optical systems," *Quantum Information and Computation* **3**, 15–37 (2003).
3. D. Porras and J.I. Cirac, "Effective quantum spin systems with trapped ions," *Physical Review Letters* **92**, 207901 (2004).
4. J.P. Barjaktarevic, G.J. Milburn, and R.H. McKenzie, "Fast simulation of a quantum phase transition in an ion-trap realisable unitary map," e-Print Archive preprint quant-ph/0401137 (22-Jan-04).
5. D.J. Berkeland, "Linear Paul trap for strontium ions," *Review of Scientific Instruments* **73**, 2856–2860 (2002).
6. T. Calarco, J.I. Cirac, and P. Zoller, "Entangling ions in arrays of microscopic traps," *Physical Review A* **63**, 062304-01–062304-20 (2001).
7. E. Dagotto and T.M. Rice, "Surprises on the way from one- to two-dimensional quantum magnets: The ladder materials," *Science* **271**, 618–623 (1996).
8. C.D. Batista and G. Ortiz, "Algebraic approach to interacting quantum systems," *Advances in Physics* **53**, 1–82 (2004).
9. M.G. Blain *et al.*, "Towards the hand-held mass spectrometer: design considerations, simulations, and fabrication of micrometer-scaled cylindrical ion traps," *International Journal of Mass Spectrometry* **236**, 91–104 (2004).
10. J.I. Cirac and P. Zoller, "New Frontiers in Quantum Information with Atoms and Ions," *Physics Today* **57**, 38–44 (March 2004).

### Acknowledgments

This work is funded through the Laboratory-Directed Research and Development program as part of 20050076DR, "Cold Atom Quantum Simulators."

For further information, contact Dana Berkeland at 505-665-9148, [djb@lanl.gov](mailto:djb@lanl.gov).



The World's Greatest Science Protecting America

Los Alamos National Laboratory, an affirmative action/equal opportunity employer, is operated by the University of California for the U.S. Department of Energy under contract W-7405-ENG-36.



# Novel Broadband Light Sources— Guiding Light through Glass and Holes

F.G. Omenetto, M.R. Wehner, M.R. Ross, E.H. Gershgoren (P-23), A.V. Efimov (MST-10), A.J. Taylor (CINT)

Over the last seven years, photonic crystal fibers (PCFs) have become one of the success stories of modern photonics.<sup>1</sup> Starting as a highly speculative idea in 1991, it is now possible to obtain PCFs in different varieties with specifically tailored features.<sup>2</sup> A typical PCF consists of an array of microscopic holes (hollow capillaries with diameters precisely controllable in the range  $\sim 25$  nm to  $\sim 50$  nm) running along the fiber length (Figure 1). These holes act as optical barriers or scatterers which, suitably arranged, can trap light within a central core (either hollow or made of solid glass). The very large air-glass refractive-index difference opens up many new possibilities not available in standard fibers. For example, light can be guided in a hollow core by a photonic-bandgap effect. The revolutionary nature of the waveguides and their very high performance measured in terms of loss, nonlinearity, and dispersion control means that applications are emerging in many diverse areas of science and technology.

## A Rainbow of Light

One of the immediate consequences of these new waveguides is the spawning of renewed interest in the study of nonlinear processes in optical fibers, specifically in regards to supercontinuum formation and various mixing and nonlinear frequency-conversion processes. A supercontinuum is formed when a short pulse of light (typically of subpicosecond duration) undergoes a nonlinear interaction with the material in which it propagates. Such interaction, in the appropriate conditions, leads to a dramatic broadening

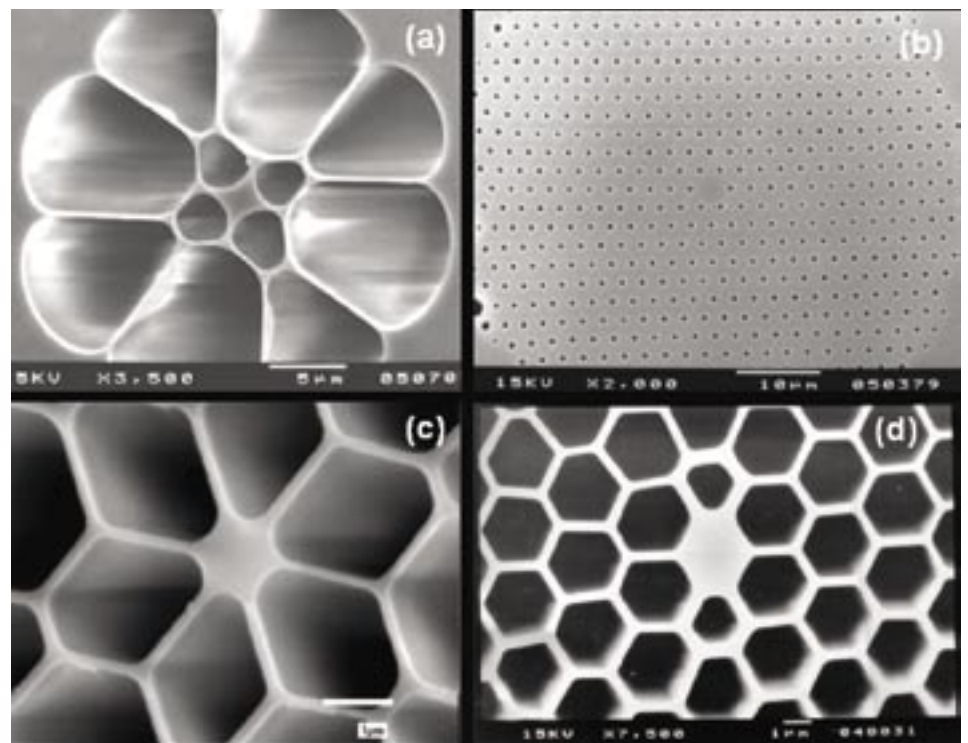


Figure 1. Scanning-electron-microscope images of the cross section of various PCF samples. Fiber (a) is the extruded soft-glass PCF used for ultrabroadband supercontinuum generation.<sup>10,11</sup> Fiber (b) is the dispersion-flattened silica PCF that allows us to obtain flat and controlled dispersion curves (close to zero dispersion over  $\sim 300$  nm).<sup>2</sup> Fibers (c) and (d) are both high air fill cladding PCF. Fiber (c) is used to generate supercontinuum with  $\lambda \sim 800$  nm short-pulse pumping and phase-matched modes in the visible and ultraviolet.<sup>3,4,7,8</sup> Fiber (d) is highly birefringent fiber for enhanced polarization dependent nonlinear effects (photo courtesy of the University of Bath).

RESEARCH HIGHLIGHT  
PHYSICS DIVISION

## Atomic Physics Research Highlights

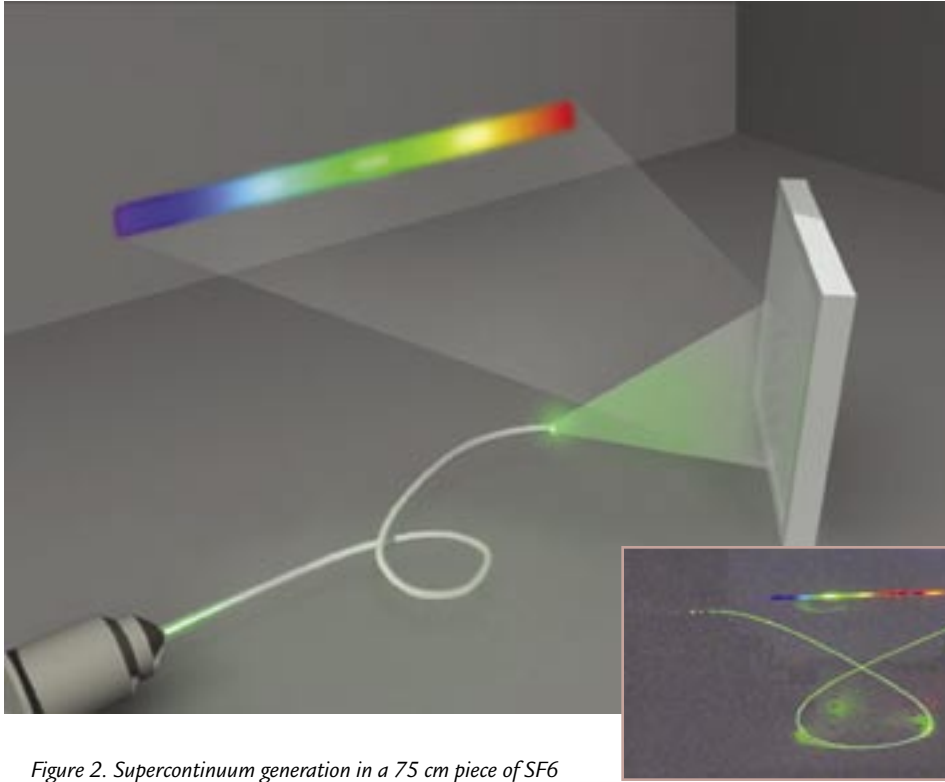


Figure 2. Supercontinuum generation in a 75 cm piece of SF<sub>6</sub> PCF. The background of the image shows the output of the fiber dispersed by a grating and focused on a white piece of paper. The visible components are generated by the nonlinear interactions that spectrally broaden the 1550 nm, 100 fs pulse coupled in the fiber.

of the pulse's bandwidth, and provides a "rainbow of colors" at the output. These conditions were traditionally obtained in the early 1980s by propagating high-intensity laser pulses through materials such as sapphire. PCFs provide the very desirable feature of confining and guiding the optical field in a glass core whose diameter does not exceed a few microns. Having a moderately high-intensity femtosecond laser pulse combined with the spatial confinement of the guided mode is enough to make the nonlinear interaction between light and glass the overwhelmingly dominant process governing pulse propagation in PCF.

Spectacular frequency-conversion phenomena occur in these conditions. We have described power-dependent generation of visible radiation by coupling femtosecond pulses at a wavelength of 1550 nm in a 95 cm segment of a "high- $\Delta$ " microstructured fiber (i.e., high-air

filling in the cladding). Two bands of visible radiation were generated by a combination of temporal pulse splitting of the fundamental pulse followed by Raman self-frequency shifting of one of the split pulses and a subsequent third harmonic generation of both frequencies.<sup>3</sup> The visible generated radiation is dependent on the polarization state of the input pulse coupled into the PCF.

One of the most dramatic manifestations of the nonlinear effects in PCFs is supercontinuum generation.<sup>4</sup> When 100 fs pulses from titanium-sapphire lasers ( $\lambda \sim 800$  nm) were coupled in a few meters of these fibers, the combination of nonlinear effects gave rise to a significant spectral broadening spanning nearly 1000 nm. This result provided a practical means to achieve an efficient pulsed white light source encompassing an "optical octave" (400–800 nm). This latter feature is of great value in realizing

precision measurement techniques based on supercontinuum frequency combs (Figure 2).

The appeal of controlling supercontinuum as a practical source of light remains very high. The availability of such a broad-bandwidth source is extremely important for a variety of applications such as spectroscopic detection and interrogation, new laser source generation, broad-bandwidth communication sources, and arbitrary signal generation. Typically made of silica, the PCFs used to generate supercontinuum radiation provide slightly in excess of one optical octave usually limited by the physical properties of the fiber itself (such as modes supported, wavelength-dependent absorption, dispersion etc.).

### Summary of Some Experimental Results

We experimentally observed that the propagation of a pulse of fixed energy, though linearly polarized along different directions, yields very distinct visible components at the output.<sup>5</sup> These results suggest a polarization-dependent selectivity for phase-matching (i.e., frequency conversion) according to the input polarization state. Such polarization-dependent selectivity provides a means to generate specific harmonics and, therefore, a means to control the output's visible frequency through the input pulse polarization state. These approaches are promising for the research and development of all-fiber signal control and in-fiber ultrafast optical switching.<sup>6</sup> Furthermore, through intramodal phase matching processes in PCFs, one can generate guided modes well into the ultraviolet region ( $\lambda < 250$  nm)<sup>7–9</sup> (Figure 3).

In collaboration with the University of Bath, we have experimented with soft Schott glass (SF6) PCFs and studied supercontinuum formation in these new structures. This glass exhibits greater transparency in the infrared than silica

and also has a higher nonlinear index of refraction, thereby enhancing the nonlinear interaction between the optical pulse and the glass. Initial results indicated a broader supercontinuum than what was conventionally achievable with silica-based PCFs, extending the spectral span to  $\sim 1400$  nm after propagating pulses in a 75 cm piece of fiber.<sup>10</sup>

We have recently demonstrated the broadest supercontinuum formation ever recorded<sup>11</sup> by propagation  $\lambda = 1550$  nm,  $\sim 100$  fs pulses of 1 nJ energy in a short ( $Z = 4.7$  mm) piece of the SF6 PCF. The measurement illustrated in Figure 4 compares a typical supercontinuum trace obtained with silica PCF. The present measurement is limited by the finite spectral sensitivity of the cooled mercury-cadmium-titanium detector, which does not go beyond 3  $\mu\text{m}$ . The extensive span of this supercontinuum offers opportunities across multiple wavelength areas, covering seven optical octaves of 400 nm, for instance, and extending the wavelength ranges well into the infrared region. In addition to the spectral extent of this source, this result has given us further insight into the physical mechanism of supercontinuum.<sup>4</sup>

## Conclusion

The study of these fibers and the nonlinear effects that take place in them is an area rich in opportunities in the basic and applied sciences. A glimpse of the breadth of the field is offered by the future possibilities that include new approaches to optical fiber sensors, high-power fiber lasers, sources for medical imaging, and hollow-core photonic crystal fibers

(which open exciting avenues to realize enhanced, specialized Raman cells for high-sensitivity spectroscopy, or for the sensing of atmospheric contaminants such as molecules or viruses).

The future looks bright for guided light.

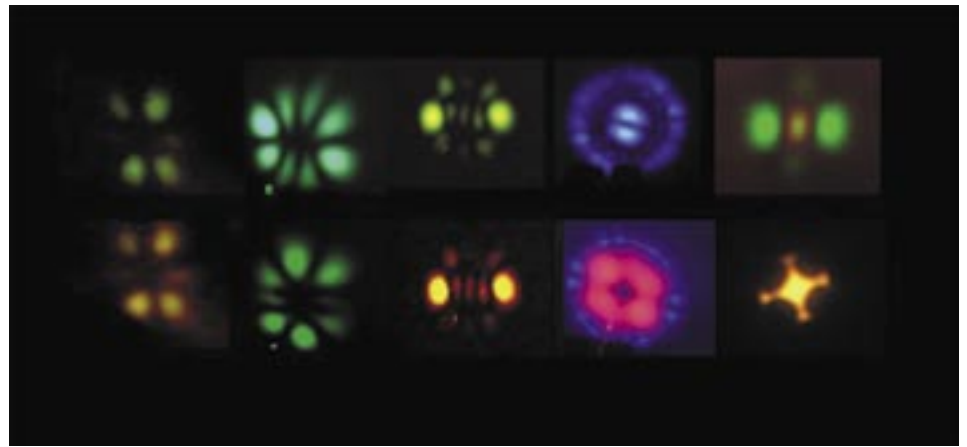
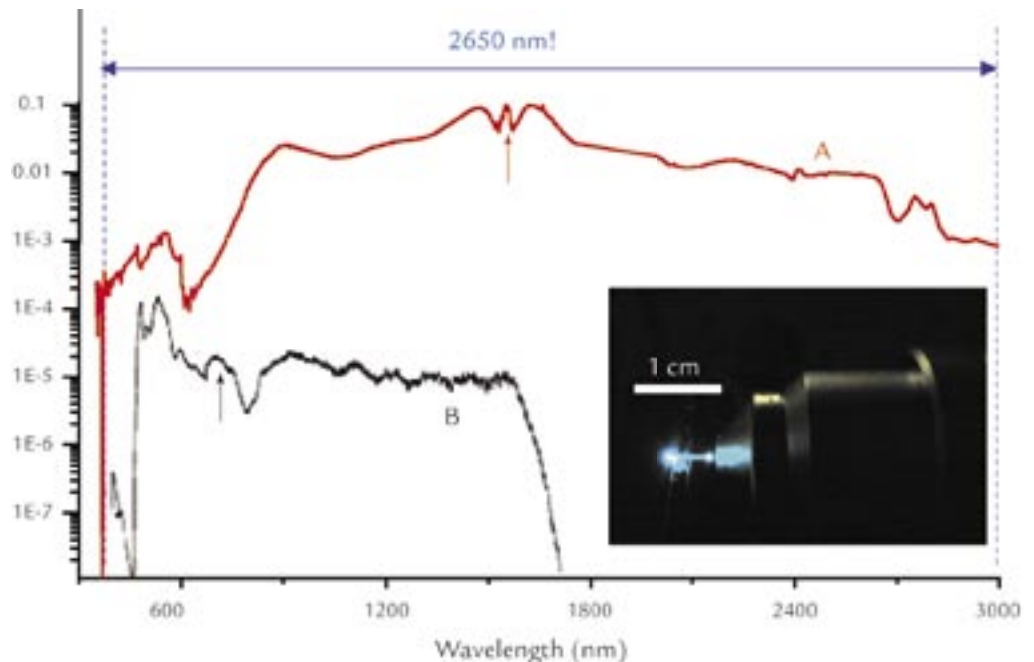


Figure 3. Far-field images of the generated, visible-guided modes resulting from frequency-conversion processes in PCFs. All of these modes are obtained by phase-matched generation of third harmonic in silica PCF with the exception of the last pair, which is generated in the SF6 fiber (for a detailed description and analysis refer to References 5–10).

Figure 4. Ultrabroad supercontinuum (curve A) generated in a  $Z = 4.7$  mm piece of SF6 PCF. Pulses used in the experiment have temporal duration of 110 fs at  $\lambda = 1550$  nm, and the energy per pulse is  $\sim 1$  nJ ( $P_{\text{avg}} = 80$  mW at an 80 MHz repetition rate). The supercontinuum average power at the output of the fiber is 20 mW. And the radiation generated spans a range from at least 350 nm to 3000 nm (the detectors used were sensitive only in this wavelength range). Curve B represents the typical supercontinuum obtained by coupling 800 nm pulses in silica PCFs (after Reference 10). The axes have been adjusted to match the scales for both cases. The arrows indicate the pumping wavelength in the two cases. The inset shows a picture of the SF6 fiber when supercontinuum is being generated. The microscope objective used for coupling the pulses is also visible.



## Atomic Physics Research Highlights

### References

1. P. Russell, "Photonic crystal fibers," *Science* **299**, 358–362 (2003).
2. W.H. Reeves *et al.*, "Supercontinuum generation in dispersion flattened photonic crystal fiber," *Nature* **424**, 511–515 (2003).
3. F.G. Omenetto *et al.*, "Polarization dependent third harmonic generation in photonic crystal fibers," *Optics Express* **11**, 61–67 (2003).
4. J.K. Ranka, R.S. Windeler, and A.J. Stentz, "Visible continuum generation in air-silica microstructure optical fibers with anomalous dispersion at 800 nm," *Optics Letters* **25**, 25–27 (2000).
5. F.G. Omenetto *et al.*, "Simultaneous generation of spectrally distinct third harmonic in photonic crystal fibers," *Optics Letters* **26**, 1558–1560 (2001).
6. F.G. Omenetto *et al.*, "Polarization dependent third harmonic generation in photonic crystal fibers," *Optics and Photonics News* **14**, 36 (2003).
7. F.G. Omenetto, "Femtosecond pulses in optical fibers," in *Progress in Optics*, E. Wolf (Ed.), (Elsevier, Amsterdam, 2002), **44**, pp. 85–141.
8. A. Efimov *et al.*, "Phase-matched third harmonic generation in microstructured fibers," *Optics Express* **11**, 2567–2576 (2003).
9. A. Efimov *et al.*, "Nonlinear generation of very high order UV modes in microstructured fibers," *Optics Express* **11**, 910–918 (2003).
10. V.V. Ravi Kanth Kumar *et al.*, "An extruded soft glass photonic crystal fiber for supercontinuum generation," *Optics Express* **10**, 1520–1525 (2002).
11. F.G. Omenetto *et al.*, "An ultrabroad supercontinuum laser source," (in preparation).

### Acknowledgment

We gratefully acknowledge our collaborators at the University of Bath (Philip Russell and Jonathan Knight) for the continuous collaboration and for the endless supply of new PCF samples, and specifically Will Reeves and V.V.R.K. Kumar for the early work on SF6 fibers. This work was funded by the Laboratory-Directed Research and Development program.

For further information, contact Fio Omenetto, 505-665-5847, omenetto@lanl.gov.



The World's Greatest Science Protecting America

Los Alamos National Laboratory, an affirmative action/equal opportunity employer, is operated by the University of California for the U.S. Department of Energy under contract W-7405-ENG-36.



# Time Variation of Alpha

J.R. Torgerson, S.K. Lamoreaux, T. Fortier, E. Gershgoren, F.G. Omenetto, M.M. Schauer (P-23), D. Budker, T. Nguyen (University of California, Berkeley), S.A. Diddams (National Institute of Standards and Technology), V.V. Flambaum (University of New South Wales)

If we accept the idea that our universe formed from nothing with the “big bang,” it must also seem reasonable that, at some point in the past, fundamental constants of physics were varying with time. Moreover, events that likely occurred immediately following the big bang, such as inflation and later acceleration, suggest a modification of the values of fundamental constants. A smooth evolution of the values of such parameters would thus lead to the conclusion that they are still changing and that this change may be measurable even today. Because our most widely accepted theories of nature do not allow for such variation, such evidence would be proof of physics beyond our current understanding. It is important to point out that there is little basis to assert that many of the parameters in our theories of nature are constants independent of space and time.

The question of whether the fundamental constants are still varying has been of interest at least since Dirac put forward his “large number hypothesis.”<sup>1</sup> Dirac noticed that certain dimensionless combinations of physical constants fell into three groups of order: unity,  $10^{40}$ , and  $10^{80}$ . The  $10^{40}$  group, in particular, was thought to depend on the size of the universe. Although this hypothesis was based on coincidental observations, the formalism of modern string theory allows for the possibility of a dependence of the fundamental constants on the gravitational potential, or possibly on the dark energy responsible for the nonzero cosmological constant.

Of particular interest for variation of fundamental constants are the

dimensionless gauge coupling constants, such as the fine-structure constant ( $\alpha = 1/137 = e^2/hc$ ) whose value determines the strength of electromagnetic interactions. Table 1 summarizes the results of some of the recent searches for time variation of  $\alpha$ . Recent astronomical observations have indicated that over the last 10 billion or so years the value of  $\alpha$  has changed and that the average rate of fractional variation is  $\dot{\alpha}/\alpha \approx 10^{-16}/\text{yr}$ ,<sup>2</sup> although this result remains controversial<sup>3</sup>. Analysis of the ancient nuclear fission reactor in Gabon, West Africa, can also be used to search for ancient variation of  $\alpha$ , and the two most recent results are listed in Table 1 and discussed below.

Recent precision laboratory clock-comparison experiments, where different atomic transitions that depend differently on  $\alpha$  are used as frequency references and are measured over a period of years, have limited the rate of variation to  $\dot{\alpha}/\alpha < 10^{-15}/\text{yr}$ .<sup>4-6</sup> The purpose of our studies is to further improve the limit on (or observe!) time variations at the level of  $10^{-18}/\text{yr}$ . For this purpose, we have started efforts which include two laboratory measurements with atomic references and a study of the Oklo natural-reactor phenomena.

## Reanalysis of the Oklo Natural Reactor

Two billion years ago, the relative isotopic fraction of uranium-235 in natural

Table 1. Status of searches for  $\alpha$  variation

	$\dot{\alpha}/\alpha$ (yr <sup>-1</sup> )	Method	Quantity	Reference
Distant	$\leq 5 \times 10^{-15}$	Re <sub>125</sub> decay	$\alpha(m_f/\Lambda_{\text{pl}})^{1/2}$	14
	$(6.4 \pm 1.4) \times 10^{-16}$	QSO spectra	$\alpha$	2
	$(0.6 \pm 0.6) \times 10^{-16}$	QSO spectra	$\alpha$	3
	$\leq 0.8 \times 10^{-17}$	Oklo reactor	$\alpha(m_f/\Lambda_{\text{pl}})^{1/2}$	8
	$-(2.3 + 0.7/-0.3) \times 10^{-17}$	Oklo reactor	$\alpha(m_f/\Lambda_{\text{pl}})^{1/2}$	10
Local	$\leq 3.7 \times 10^{-14}$	H ↔ Hg <sup>+</sup>	$g_H/g_P \cdot \alpha^{2.2}$	15
	$\leq 1.2 \times 10^{-15}$	opt-Hg <sup>+</sup> ↔ Cs	$g_C/m_f/m_P \cdot \alpha^{5.0}$	4
	$(-0.04 \pm 1.6) \times 10^{-15}$	Rb ↔ Cs	$g_C/g_N \cdot \alpha^{0.44}$	5
	$(-0.3 \pm 2.0) \times 10^{-15}$	Opt-Yb <sup>+</sup> ↔ Cs	$g_C \cdot m_f/m_P \cdot \alpha^{2.0}$	6

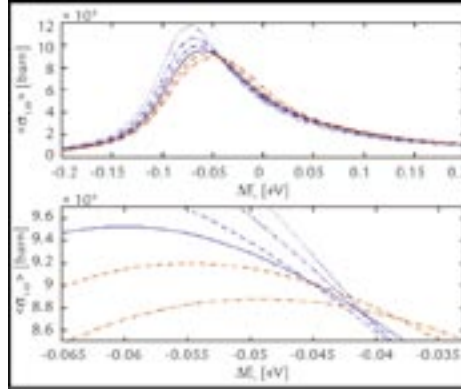
# RESEARCH HIGHLIGHT

# PHYSICS DIVISION



## Atomic Physics Research Highlights

Figure 1. Calculation of the neutron-absorption cross section for  $^{149}\text{Sm}$   $\hat{\sigma}_{149} \equiv \langle \sigma_{149} \rangle$  as a function of change in resonance energy  $E_r$ , and as a function of temperature for  $\Sigma_a/\Sigma_s = \sqrt{300/T}$ , where  $\Sigma_a$  and  $\Sigma_s$  are total neutron-absorption and -scattering cross sections, respectively. Blue dots: 300 K; blue dot-dash: 400 K; blue dashes: 500 K; solid blue: 600 K; red dashes: 700 K; and red dot-dash: 800 K. The measured value for  $\hat{\sigma}_{149} \approx 90$  kb, which suggests that  $E_r$  has shifted towards larger values since Oklo was an active reactor.



uranium was 3.7% compared to the present value of 0.7%. It is not possible to have a self-sustained nuclear chain reaction with a homogeneous mixture of water and uranium with isotopic composition at the 0.7% level. However, with 3.7% enrichment, it is possible to attain a neutron multiplication factor of about 1.38 with 2.4 water molecules per uranium atom. As suggested by P. Kuroda in 1956, if an ancient uranium ore deposit was sufficiently concentrated, saturated with water, and had a low concentration of neutron absorbers, an ore deposit could become a natural nuclear reactor.

The remnants of such a natural reactor were discovered in Gabon, Africa, in 1972 during routine analysis of uranium samples. (With the exception of lead and helium, the isotopic composition of the chemical elements in the Earth's crust is so constant that deviations are used to identify, for example, rocks from Mars that have ended up on Earth.) This natural reactor ran for about 100,000 years, two billion years ago, and the ore deposit and reactor products were preserved in an extremely stable geological formation. Subsequent isotopic analysis, after correcting for influx of natural isotopic-abundance chemical elements, matches the isotopic composition of spent fuel from modern nuclear reactors.

Shlyachter<sup>7</sup> pointed out that it is possible to test for a variation in  $\alpha$  (or other parameters that determine nuclear energy levels) by determining fission fragment concentrations for isotopes that have a low-energy neutron absorption resonance

due to the strong energy dependence of the low-energy neutron population.

Two analyses of samples from the Oklo deposit indicated no variation of the resonance energy and yielded an upper limit for the fractional variation of  $\alpha$  at the  $10^{-17}/\text{yr}$  level.<sup>8,9</sup> However, in addition to the total neutron flux and the location of the resonance, the specific spectrum of the neutron flux is important. The previous analyses assumed a Maxwell-Boltzmann spectrum, known to be incorrect in the presence of absorbers (which include uranium and water, which formed the basis of the reactor). We repeated the analysis with a more realistic neutron spectrum and found  $\dot{\alpha}/\alpha \geq 2.3 \times 10^{-17}/\text{yr}$  with  $8\sigma$  confidence.<sup>10</sup> A result of our analysis is shown in Figure 1. This result is about ten times smaller than the astrophysical result<sup>2</sup> and of opposite sign; both the magnitude and sign of the variation can be accommodated in modern theories of the universe.<sup>11</sup> Our result was covered as a feature article in *New Scientist*.<sup>12</sup>

### Comparison of Optical Frequency References

Although laboratory measurements do not have the advantage of integrating over  $10^9$ – $10^{10}$  years, they provide significant conveniences—they can be made in a carefully prepared environment and are reproducible. Furthermore, the resolution on parameters of interest can be increased by a large factor which can allow a measurement with higher precision but on a laboratory time scale. Laboratory

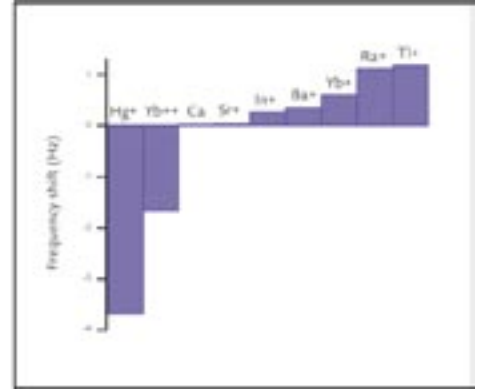


Figure 2. Frequency shift of proposed optical references for a fractional shift  $\Delta\alpha/\alpha = 10^{-15}$ .

measurements are also sensitive to short-time variations and to possible spatial and gravitational dependencies.

Because  $\alpha$  determines the strength of electromagnetic interactions, the energies of atomic states depend upon  $\alpha$ . Moreover, different states have different dependencies on  $\alpha$  primarily due to relativistic corrections to the energies. That these corrections can be calculated accurately is the basis for nearly all ideas regarding laboratory measurements of  $\alpha$  variation.

Twenty-five years ago, Hans Dehmelt recognized that group-III A ions, in particular, indium and thallium ( $\text{In}^+$  and  $\text{Tl}^+$ ), would be excellent choices on which to base atomic clocks of unprecedented stability. By the same fundamental considerations, we recently identified a ytterbium ion ( $\text{Yb}^{2+}$ ) as another promising candidate. These atomic ions possess metastable energy states that decay back to the ground state. This transition is insensitive to fluctuating ambient fields and the transition frequency is  $\sim 10^{15}$  Hz (in the optical regime), which improves the short-term stability of a reference based upon it. In addition, atomic ions can be trapped and cooled until they are nearly motionless unlike clouds of neutral atoms that suffer from systematic collisional effects and are not trapped. These ions were chosen as candidates for this effort because these “clock” transitions are some of the most  $\alpha$  sensitive (Figure 2). We are

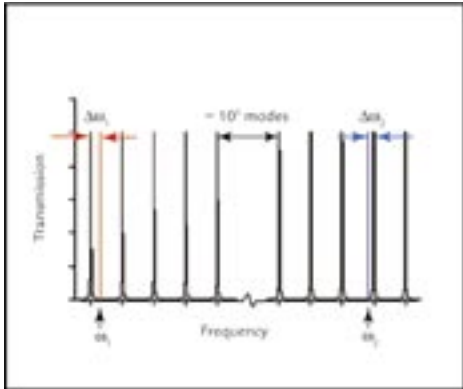


Figure 3. Mode population for the OCR or OFC as a function of frequency. Light from optical references is shown in red ( $\omega_1$ ) and blue ( $\omega_2$ ).

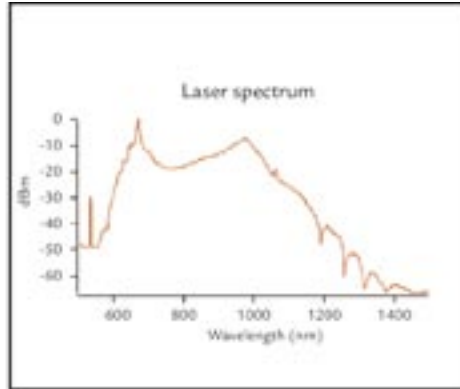


Figure 4. Light output from the “GHz” optical comb generator. The spectrum consists of extremely well defined spectral components separated by 500 MHz (not resolved on this plot).

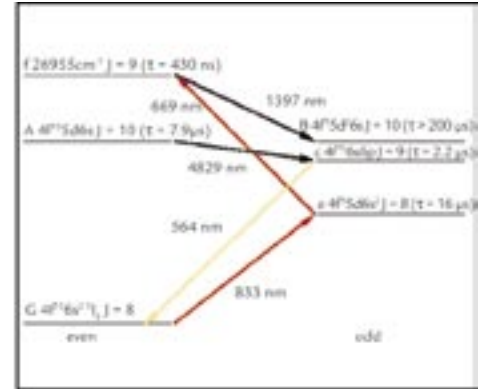


Figure 5. Partial Grotrian diagram for dysprosium. The levels of interest for a search for variation in  $\alpha$  are labeled A and B.

currently constructing an ion-trapping/-imaging apparatus for spectroscopy of both indium(+) and ytterbium(2+) as the first step towards our goal of comparing all three. A measurement with these three ions has the potential to achieve a sensitivity of  $\delta(\dot{\alpha}/\alpha) \approx 10^{-18}/\text{yr}$  with a measurement time of one year. This is over 1000 times more sensitive than current laboratory measurements.

We are constructing narrow-band laser sources to probe the metastable transitions, thereby creating accurate ion-stabilized optical frequency references. Other transitions from the ground state are strong enough to be used to optically cool the ions and serve as “readout” transitions to determine the electronic states of the ions.

One of the main obstacles in performing an experiment to compare frequency references in which at least one of the references is optical is that the appropriate high-speed electronics do not exist to directly measure the  $10^{14}$ – $10^{15}$  Hz frequency. However, our experiment does not require accurate knowledge of the frequencies of the references, or even the difference frequency. It is sufficient to measure changes in the difference of frequencies of relatively stable atomic references to measure changes in  $\alpha$ . It is this fact that makes this experiment feasible with existing experimental methods.

We will use two existing technologies—the optical comparison resonator (OCR) and the femtosecond optical frequency comb (OFC)—to make redundant measurements to verify our results. The underlying concept is illustrated in Figure 3 and is similar for both the OCR and OFC although its implementation differs. For the OCR, the ion-stabilized frequency references are shifted into resonance with passive optical resonator modes, and the frequencies shift is measured. For the OFC, the stable references beat with populated modes emitted from the OFC laser source and the beat frequency is measured.

The OFC relies on a broadband, mode-locked laser. When operated in the mode-locked regime, the output of the laser consists of well-defined pulses whose repetition frequency is the free spectral range (FSR) of the laser resonator. The spectral components of the output are then separated by the FSR and span the fraction of the gain bandwidth of the laser over which dispersion is compensated. With our collaborators at the National Institute of Standards and Technology

(NIST), we have constructed a titanium-doped sapphire laser with an FSR of 500 MHz and a spectrum covering more than an octave centered at about 800 nm (Figure 4). This spectral region easily includes wavelengths of interest for indium(+), thallium(+), and ytterbium(2+) optical frequency references and is sufficient to allow accurate stabilization without additional noisy measurements. We are currently working to stabilize the spectrum of this laser and understand its subtleties.

### Atomic Dysprosium

We are also conducting an experiment at the University of California (UC), Berkeley, which takes advantage of a

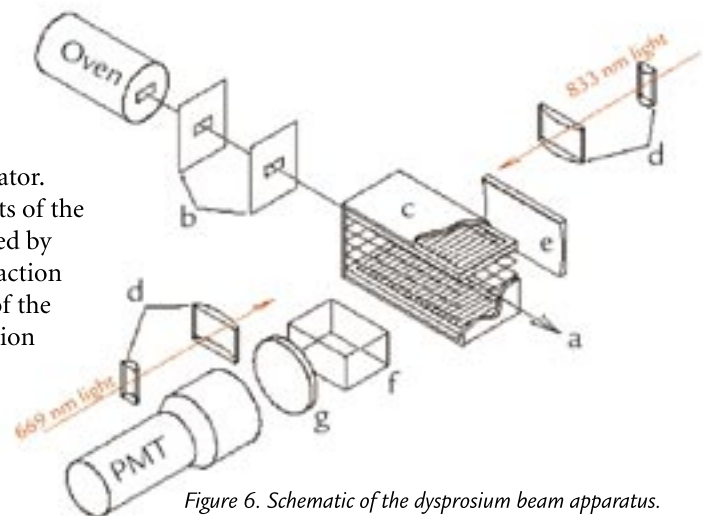


Figure 6. Schematic of the dysprosium beam apparatus.

## Atomic Physics Research Highlights

fortunate near degeneracy of two energy levels in atomic dysprosium.<sup>13</sup> As shown in Figure 5, two states of opposite parity are separated by as little as 300 MHz for a particular isotope (and by as much as 1 GHz for other isotopes). Careful mathematical modeling of these levels has been conducted due to interest in these states for measurements of parity nonconservation, and the states have been determined to be nearly as sensitive to variations of  $\alpha$  as ytterbium(2+). Although optical transitions offer advantages for frequency references, a measurement of  $\alpha$  variation does not require the use of two separated references.

The advantage of this system over others is that the frequency measurements have been reduced from optical frequencies to radio frequencies, which can be monitored with well-developed techniques. A determination of a fractional shift of  $\dot{\alpha}/\alpha \approx 10^{-18}$  requires an uncertainty  $\delta\nu \approx 1$  mHz. This is a fractional uncertainty of only  $\delta\nu/\nu \approx 10^{-12}$ , which can be achieved with a commercially available radio-frequency reference, such as that derived from a cesium beam standard.

A schematic of the apparatus currently in use at UC-Berkeley is shown in Figure 6. The apparatus is essentially a simple radio-frequency atomic “clock” based upon a dysprosium beam and possessing a single interaction region. The transition between states A and B can be addressed with an applied electric field at the appropriate frequency. Spectroscopy on this transition is performed by monitoring the fluorescence of the atoms at 564 nm. We are currently studying several systematics that can affect the sensitivity of our measurements for tests of  $\alpha$  variation.

## References

1. P.A.M. Dirac, *Nature* **139**, 323 (1937).
2. M.T. Murphy *et al.*, “Possible evidence for a variable fine-structure constant from QSO absorption lines: motivations, analysis and results,” *Monthly Notices of the Royal Astronomical Society* **327**, 1208–1222 (2001); J.K. Webb *et al.*, “Further evidence for cosmological evolution of the fine-structure constant,” *Physical Review Letters* **87**, 091301-1–091301-4 (2001).
3. R. Srianand *et al.*, “Limits on the time variation of the electromagnetic fine structure constant in the low energy limit from absorption lines in the spectra of distant quasars,” *Physical Review Letters* **92**, 121302-1–121302-4 (2004).
4. S. Bize *et al.*, “Testing the stability of fundamental constants with the <sup>199</sup>Hg<sup>+</sup> single-ion optical clock,” *Physical Review Letters* **90**, 150802-1–150802-4 (2003).
5. H. Marion *et al.*, “Search for variations of fundamental constants using atomic fountain clocks,” *Physical Review Letters* **90**, 150801-1–150801-4 (2003).
6. E. Peik *et al.*, “New limit on the present temporal variation of the fine structure constant,” *Physical Review Letters* **93**, 170801-1–170801-4 (2004).
7. A.I. Schlyakter, *Nature* **264**, 340 (1976).
8. Y. Fujii *et al.*, “The nuclear interaction at Oklo 2 billion years ago,” *Nuclear Physics B* **573**, 377–401 (2000).
9. T. Damour and F. Dyson, “The Oklo bound on the time variation of the fine-structure constant revisited,” *Nuclear Physics B* **480**, 37–54 (1996).
10. S.K. Lamoreaux and J.R. Torgerson, “Neutron moderation in the Oklo natural reactor and the time variation of alpha,” *Physical Review D* **69**, 121701-1–121701-5 (2004).
11. D.F. Mota and J.D. Barrow, “Local and global variations of the fine-structure constant,” *Monthly Notices of the Royal Astronomical Society* **349**, 291–302 (2004).
12. E.S. Reich, “Speed of light may have changed recently,” *New Scientist*, 3 July 2004 (No. 2454), pp. 6–7.
13. A.T. Nguyen *et al.*, “Towards a sensitive search for variation of the fine-structure constant using radio-frequency E1 transitions in atomic dysprosium,” *Physical Review A* **69**, 022105-1–022105-8 (2004).
14. F.J. Dyson, “The fundamental constants and their time variation” in *Aspects of Quantum Theory*, A. Salam and E.P. Wigner, Eds. (Cambridge University Press, Cambridge, 1972), pp. 213–236.
15. J.D. Prestage, R.L. Tjoelker, and L. Maleki, “Atomic clocks and variations of the fine structure constant,” *Physical Review Letters* **74**, 3511-3514 (1995).

## Acknowledgment

We would like to thank our LANL management for their ongoing support of our efforts. This work is currently funded through the LANL Laboratory Directed Research and Development program, the UC/LANL Campus-Laboratory Collaborations Program and by a NIST Precision Measurements Grant.

For further information, contact Justin Torgerson, 505-665-3365, [torgerson@lanl.gov](mailto:torgerson@lanl.gov).



The World's Greatest Science Protecting America

Los Alamos National Laboratory, an affirmative action/equal opportunity employer, is operated by the University of California for the U.S. Department of Energy under contract W-7405-ENG-36.

